

SECRET  
CONFIDENTIAL

NACA RM E54C09

204  
Copy  
RM E54C09

TECH LIBRARY KAFB, NM

0143297



# RESEARCH MEMORANDUM

GL89

ANGLE - OF - ATTACK SUPERSONIC PERFORMANCE OF A  
CONFIGURATION CONSISTING OF A RAMP - TYPE SCOOP  
INLET LOCATED EITHER ON TOP OR BOTTOM  
OF A BODY OF REVOLUTION

By Emil J. Kremzier and Robert C. Campbell

Lewis Flight Propulsion Laboratory  
Cleveland, Ohio  
(Classification code: A-1, C-10, Under Sec. 1 F-6)  
By: NASA Tech Pub Announcement #8  
(Former AFIB#1: U CHANGE)

By ..... 26 Aug. 59.

NK

GRADE OF OFFICER MAKING CHANGE)

9 Mar. 61 CLASSIFIED DOCUMENT

This material contains information affecting the National Defense of the United States within the meaning of the espionage laws, Title 18, U.S.C., Secs. 793 and 794, the transmission or revelation of which in any manner to an unauthorized person is prohibited by law.

NATIONAL ADVISORY COMMITTEE  
FOR AERONAUTICS

WASHINGTON

May 13, 1954

CONFIDENTIAL



0143297

NACA RM E54C09

## NATIONAL ADVISORY COMMITTEE FOR AERONAUTICS

RESEARCH MEMORANDUM

## ANGLE-OF-ATTACK SUPERSONIC PERFORMANCE OF A CONFIGURATION

CONSISTING OF A RAMP-TYPE SCOOP INLET LOCATED EITHER

ON TOP OR BOTTOM OF A BODY OF REVOLUTION

By Emil J. Kremzier and Robert C. Campbell

## SUMMARY

CU-1  
3227

An investigation to evaluate the relative merits of locating a ramp-type scoop inlet either on top or bottom of a body of revolution was conducted in the Lewis 8- by 6-foot supersonic wind tunnel at Mach numbers from 1.5 to 2.0 for a range of angles of attack and inlet mass-flow ratios.

Results of the investigation indicated that changing the inlet location from the bottom to the top of the fuselage at angle of attack decreased both configuration drag and inlet pressure recovery. Resultant thrust-minus-drag for a typical turbojet-engine installation was greater for the top inlet at a given angle of attack. However, favorable and unfavorable lift interference for the bottom and top inlets, respectively, resulted in superior thrust-minus-drag performance for the bottom inlet at a given lift coefficient for most of the range of the investigation.

Comparison of top- and bottom-inlet performance for a complete aircraft configuration with a typical turbojet-engine installation yielded thrust-minus-drag results similar to that of the inlet and fuselage combination.

## INTRODUCTION

In the design of an aircraft employing an air-breathing engine, the air induction system is required to supply the prescribed air flow to the engine at high pressure recovery with as little drag as possible for efficient propulsive operation. If a fuselage scoop-type inlet is employed, body crossflow phenomena at angle of attack complicate entrance flow conditions for various circumferential inlet locations (ref. 1).

Boundary-layer thickening and crossflow separation exist on the leeward side or top surface of the fuselage at positive angles of attack and result in large regions of low-energy air. Consequently, sizable reductions in pressure recovery are incurred by inlets located on this surface. On the bottom surface, however, the boundary layer is relatively thin at angle of attack due to favorable crossflow effects, and the pressure recovery of inlets located in this region is not adversely affected. The bottom of the fuselage also acts as a compression surface at angle of attack and, as a result, may even have a favorable effect on inlet pressure recovery. In reference 1, in which the performance of conical supersonic scoop inlets on circular fuselages is reported, the drag of the bottom-inlet configuration was considerably higher than that for the top inlet.

3227

In order to evaluate the relative merits of a top or bottom installation, an investigation of a ramp-type scoop inlet successively located on the top and bottom of a body of revolution was conducted in the Lewis 8- by 6-foot supersonic wind tunnel. The scope of the investigation included free-stream Mach numbers from 1.5 to 2.0, angles of attack from zero to  $10^{\circ}$ , and a range of inlet mass-flow ratios.

#### SYMBOLS

The following symbols are used in this report:

$C_D$  drag coefficient,  $D/q_0 S_m$   
 $C_L$  lift coefficient,  $L/q_0 S_m$   
 $C_M$  pitching-moment coefficient about body station 45, moment/ $q_0 S_m l$   
D drag  
F internal thrust of turbojet engine and inlet combination  
 $F_i$  internal thrust of turbojet engine and inlet combination for  
100 percent inlet total-pressure recovery  
h boundary-layer scoop height  
L lift  
l body length, 73.125 in.  
M Mach number

$m_2/m_0$  mass-flow ratio, unity when free-stream tube as defined by cowl lip enters inlet

P total pressure

p static pressure

$q_0$  free-stream dynamic pressure,  $\gamma p_0 M_0^2/2$

$r_b$  local body radius

$r_i$  inlet radius for model of ref. 2

$S_m$  force coefficient reference area for model investigated or maximum cross-sectional area of model, 33.41 sq in.

x local body station measured from nose of body

$\alpha$  angle of attack, deg

$\gamma$  ratio of specific heats

Subscripts:

0 free stream

2 diffuser discharge

#### APPARATUS AND PROCEDURE

A sketch of the model investigated with pertinent dimensions is shown in figure 1. The fuselage consisted of the NACA RM-10 missile.

A two-dimensional 14° ramp-type inlet was mounted on the fuselage at station 45, the station of maximum diameter, and was successively located on the top and bottom of the fuselage. Details of the inlet including the subsonic diffuser are shown in figure 2. Capture area of the inlet was 3.35 square inches or approximately 11.8 percent of the basic fuselage frontal area. The inlet was designed so that the oblique shock generated by the leading edge of the 14° ramp would fall slightly ahead of the cowl lip at a Mach number of 2.0 and so that the initial internal cowl-lip angle was essentially parallel to the local flow direction behind the oblique shock. The shape of the duct cross section varied from approximately rectangular at the entrance to circular at the exit as shown in figure 2. A constant-area section

approximately  $1\frac{1}{2}$  hydraulic diameters in length was employed near the cowl lip. Area variation of the duct is shown in figure 3.

The boundary-layer air was bypassed around the inlet by positioning the ramp surface radially outward from the fuselage at a distance of 0.40 inch and inserting a wedge-shaped spacer of  $16^\circ$  included angle between the ramp and the fuselage surface. The leading edge of the wedge was located 0.80 inch downstream of the leading edge of the ramp as shown in figure 2. The wedge-spacer height chosen was approximately equal to the boundary-layer thickness at zero angle of attack, as determined from preliminary flow surveys.

Inlet mass flow was varied by means of a remotely controlled movable tail-pipe plug attached to the sting support. The model was attached to the sting by a 3-component internal strain-gage balance with its moment center located at fuselage station 45. Axial force, normal force, and pitching moment were measured by the strain-gage balance. Plug forces were not included in the balance measurements since the plug was mounted independent of the model. Base, sting, and internal thrust forces have also been excluded from the force and moment coefficients presented in the report. Internal thrust forces were obtained from the difference in momentum between the diffuser exit and the free stream.

Pressure instrumentation consisted of a 19-tube total-pressure rake and six wall static orifices located at fuselage station 66.5 just downstream of the diffuser-discharge station, four base-pressure orifices, and two chamber-pressure orifices located in the model balance cavity.

Inlet mass-flow ratio was determined from the diffuser-discharge Mach number and average total pressure. The diffuser-discharge Mach number was obtained from the known area ratio between the diffuser-discharge station and the exit plug, which was assumed to be choked. Average total pressure was calculated by area weighting the total-pressure measurements.

The investigation was conducted for a range of inlet mass-flow ratios at free-stream Mach numbers of 1.5, 1.8, and 2.0, and angles of attack of zero,  $3^\circ$ ,  $6^\circ$ , and  $10^\circ$ . Average Reynolds number for the investigation was approximately  $28.0 \times 10^6$  based on fuselage length.

## RESULTS AND DISCUSSION

### Basic Model Data

Model lift, drag, and pitching-moment coefficients for both configurations (top and bottom inlets) are shown in figure 4 as a function of angle of attack for three free-stream Mach numbers and supercritical

inlet operation. At zero angle of attack, the assymmetrical inlet and fuselage interference resulted in negative lift for the top-inlet configuration and positive lift for the configuration with the inlet on the bottom. The lift-curve slopes were about the same for both configurations for angles of attack up to  $6^{\circ}$ . Above  $6^{\circ}$ , however, the lift-curve slope became less for the configuration with the inlet on top than that for the inlet on the bottom. The top-inlet configuration also had a lower angle-of-attack drag rise than that observed for the bottom inlet.

At zero angle of attack, the effect of assymmetry of the model was to produce a negative value of pitching-moment coefficient with the inlet on the bottom and a positive value with the inlet on top. Differences in the pitching-moment coefficient between the top- and bottom-inlet configurations were small, however, for angles of attack up to  $6^{\circ}$ . Above  $6^{\circ}$  the differences became greater. The slope of all the pitching-moment curves was positive about the reference-moment center.

Inlet total-pressure recovery and model drag coefficient as a function of mass-flow ratio for four angles of attack and three free-stream Mach numbers are shown in figure 5 for the top- and bottom-inlet configurations. For the top inlet (figs. 5(a) to (c)), the critical pressure recovery and mass-flow ratio decreased significantly with increasing angle of attack, while the increase in drag coefficient was small for angles up to  $6^{\circ}$ . Critical pressure recovery and mass-flow ratio for the bottom inlet (figs. 5(d) to (f)) increased slightly with angle of attack except at a free-stream Mach number of 1.5, while a large increase in drag coefficient was observed.

#### Evaluation of Configuration Performance

Variation of inlet pressure recovery and ratio of actual thrust to ideal thrust with angle of attack are shown in figure 6 for three free-stream Mach numbers. A typical turbojet engine matched to the inlet at a diffuser-discharge Mach number of 0.20 and operating at a 35,000-foot altitude was assumed. The pressure recovery remained essentially constant or increased slightly with angle of attack for the bottom inlet but decreased rapidly with increasing angle of attack for the top inlet. Since the internal thrust of a propulsion system employing a turbojet engine is directly proportional to the pressure recovery of the inlet, the thrust ratio  $F/F_i$  had the same trend with angle of attack as the inlet pressure recoveries. Consequently, if only the inlet pressure recovery is considered, the internal thrust capabilities of a turbojet propulsion system are far greater for the bottom inlet than for the top-inlet configuration.

The excess thrust available from a given configuration, however, depends not only on the internal thrust capabilities of the propulsion system, but also on the amount of associated external drag. Thus, if an increase in configuration internal thrust is obtained at the expense of a large increase in drag, the excess thrust  $F-D$  may actually decrease, with a resultant penalty in configuration performance.

In order to compare the excess thrust of the top- and bottom-inlet configurations, the variation of  $(F-D)/F_i$  with angle of attack is presented in figure 7 for three free-stream Mach numbers. The excess thrust of the top-inlet configuration was generally higher or comparable with that of the bottom inlet at a given angle of attack. A similar result was observed in the investigation reported in reference 1.

3227

A more realistic comparison of excess thrust of a top-inlet and bottom-inlet installation would be based on a given lift coefficient rather than a given angle of attack. As discussed in the preceding section, the bottom-inlet configuration had considerably more lift than the top-inlet configuration at a given angle of attack because of the favorable and unfavorable lift interference of the bottom and top inlets, respectively. If the two configurations were to operate at comparable lift coefficients, the angle of attack of the top-inlet configuration would be increased beyond that for the bottom-inlet configuration. This increase in angle of attack would be accompanied by an increase in drag and a decrease in inlet pressure recovery with a resulting decrease in  $(F-D)/F_i$ . In order to compare the two configurations at a given lift coefficient,  $(F-D)/F_i$  as a function of lift coefficient is presented in figure 8 for a diffuser-discharge Mach number of 0.20 at three free-stream Mach numbers. Except for a limited range of lift coefficients at a Mach number of 2.0, values of  $(F-D)/F_i$  for the bottom inlet are higher than those for the top inlet at a given value of lift coefficient.

On a complete aircraft configuration, most of the lift would be supplied by a wing, with only a small portion being carried by the inlet and fuselage combination. The percentage of the complete-aircraft-configuration lift represented by the amount of inlet lift interference obtained in this investigation is unknown, but would probably be small. Consequently, the change in angle of attack that would be necessary for a complete aircraft to compensate for the change in lift produced by changing the location of the inlet from the bottom to the top of the fuselage would not be as great as that required for this investigation. Thus it is possible that, for a complete aircraft configuration,  $(F-D)/F_i$  of a top inlet may compare more favorably with a bottom inlet than was indicated in figure 8 for this investigation.

3227  
Values of  $(F-D)/F_i$  for a complete aircraft configuration were calculated from the model data of reference 2 and are presented in figure 9 as a function of trim lift coefficient for a free-stream Mach number of 2.0. A typical turbojet engine operating at a 35,000-foot altitude with an inlet diffuser-discharge Mach number of 0.18 was assumed for the calculations. The model was designed for operation with the inlet on the bottom, but negative-angle-of-attack data permitted simulation of operation with the inlet on top. From the figure,  $(F-D)/F_i$  for the bottom inlet is greater than that for the top inlet at a given value of trim lift coefficient. At a given angle of attack, however,  $(F-D)/F_i$  is greater for the top inlet than for the bottom inlet as shown by the lines in the figure connecting equal values of angle of attack. Thus, the comparison of  $(F-D)/F_i$  for the top and bottom inlets of the complete aircraft configuration is similar to that observed for the inlet and fuselage configuration of this investigation. It should be pointed out that the fuselage of the model of reference 2 had a flat-bottomed section just ahead of the inlet which, for operation with the inlet on the bottom, formed an effective compression surface for the entering flow, particularly at positive angles of attack. With the inlet on top (model inverted), the flat section would lose its effectiveness as a compression surface at positive angles of attack and may even be detrimental to inlet performance. Consequently, the model is not necessarily considered a sound design for operation with the inlet on top.

Although the data presented herein generally indicated superior performance for the bottom inlet at a given lift coefficient, the top inlet was generally superior at a given angle of attack. As discussed previously in this section, the change in angle of attack necessary for a complete aircraft to compensate for the change in lift produced by changing the location of the inlet from the bottom to the top of the fuselage is not as great as that required for the inlet and fuselage configuration. If the inlet lift interference becomes very small in proportion to the lift supplied by the wing, the  $(F-D)/F_i$  variation will approach that shown in figure 7 for angle of attack where the top inlet is comparable or superior to the bottom inlet.

#### SUMMARY OF RESULTS

An investigation was conducted to obtain a performance comparison of a ramp-type scoop inlet located either on top or bottom of a body of revolution at Mach numbers from 1.5 to 2.0, and the following results were obtained:

1. At angle of attack, changing the inlet location from the bottom to the top of the fuselage decreased both configuration drag and inlet pressure recovery.

2. In terms of thrust-minus-drag for a typical turbojet-engine installation, the top inlet was slightly superior to the bottom inlet at a given angle of attack.

3. Because of favorable and unfavorable lift interference for the bottom and top inlets, respectively, the thrust-minus-drag performance of the bottom inlet was generally superior to that of the top inlet at comparable lift coefficients for all but the lower values of lift coefficient.

4. Comparison of top- and bottom-inlet performance for a complete aircraft configuration having a fuselage scoop-type inlet and a typical turbojet-engine installation yielded results similar to that of the inlet and fuselage combination.

Lewis Flight Propulsion Laboratory  
National Advisory Committee for Aeronautics  
Cleveland, Ohio, March 11, 1954

3227

## REFERENCES

1. Hasel, Lowell E.: The Performance of Conical Supersonic Scoop Inlets on Circular Fuselages. NACA RM L53I14a, 1953.
2. Fradenburgh, Evan A., and Campbell, Robert C.: Characteristics of a Canard-Type Missile Configuration with an Underslung Scoop Inlet at Mach Numbers from 1.5 to 2.0. NACA RM E52J22, 1953.

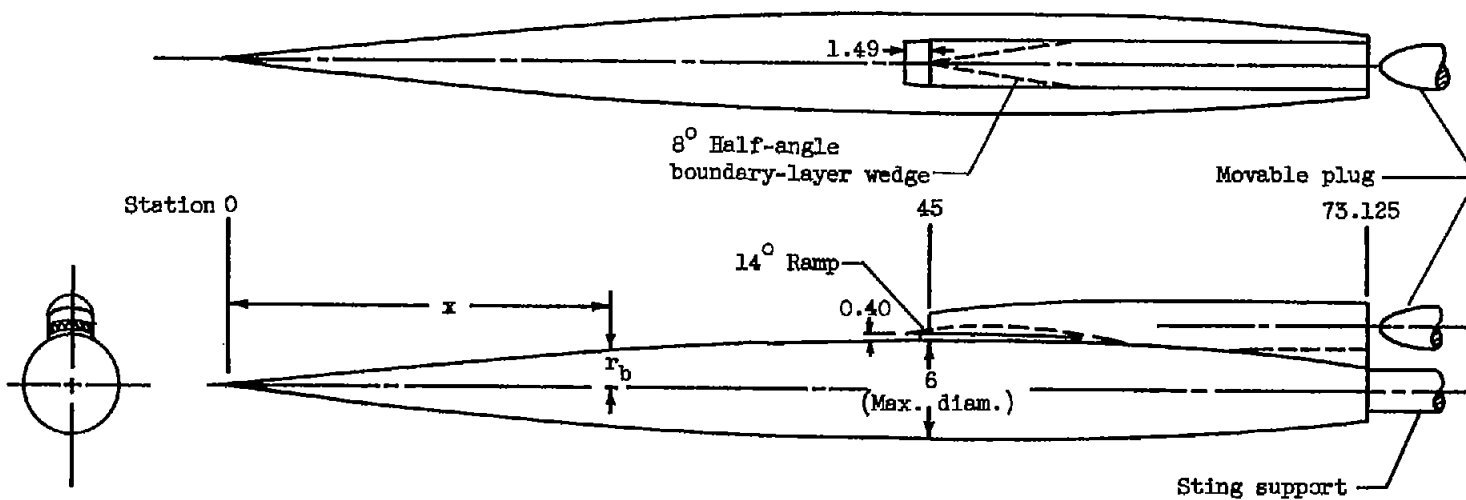


Figure 1. - Sketch of model investigated. Body defined by  $r_b = \frac{x}{15} (2 - \frac{x}{45})$ . (Dimensions are in inches.)

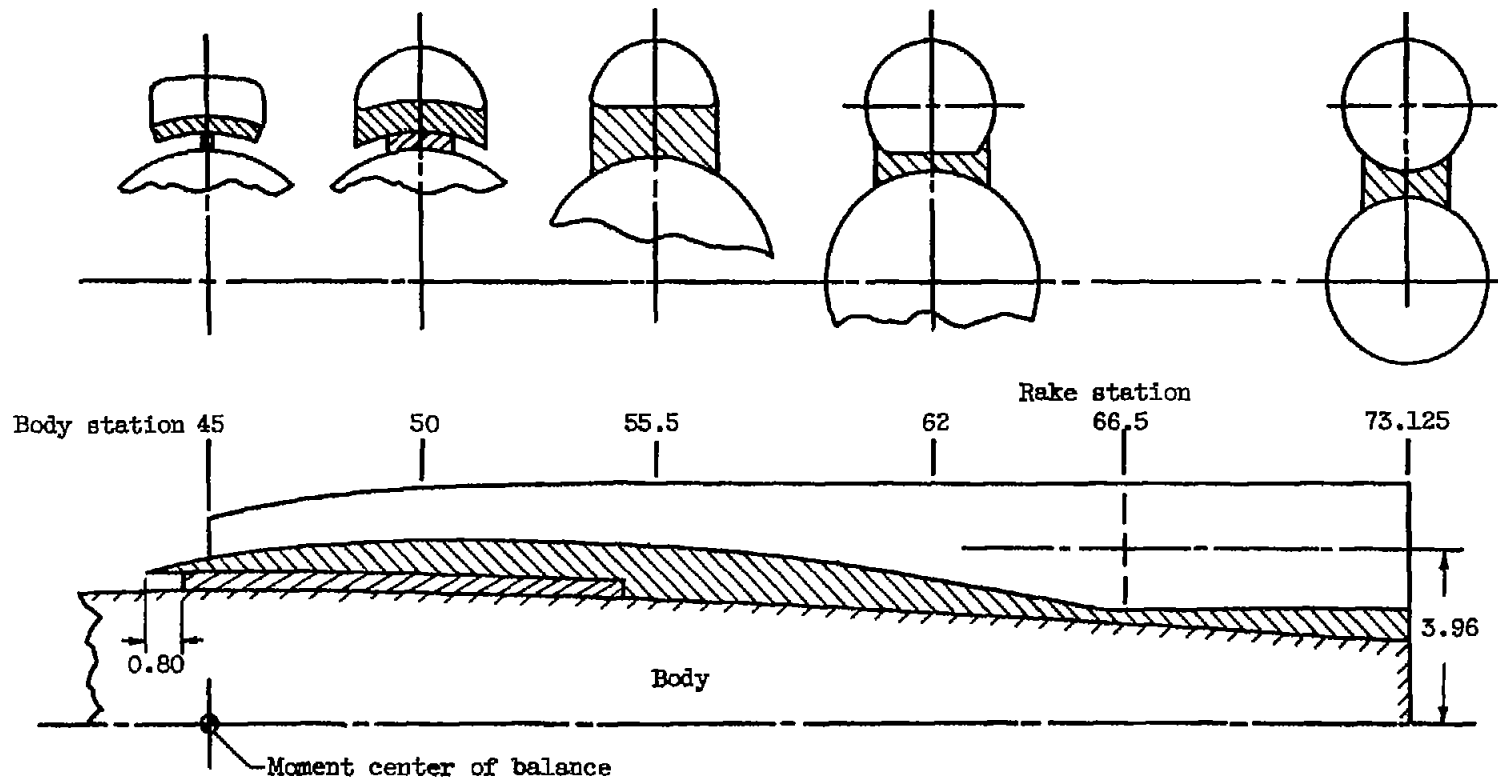


Figure 2. - Details of inlet. (Dimensions are in inches.)

3227

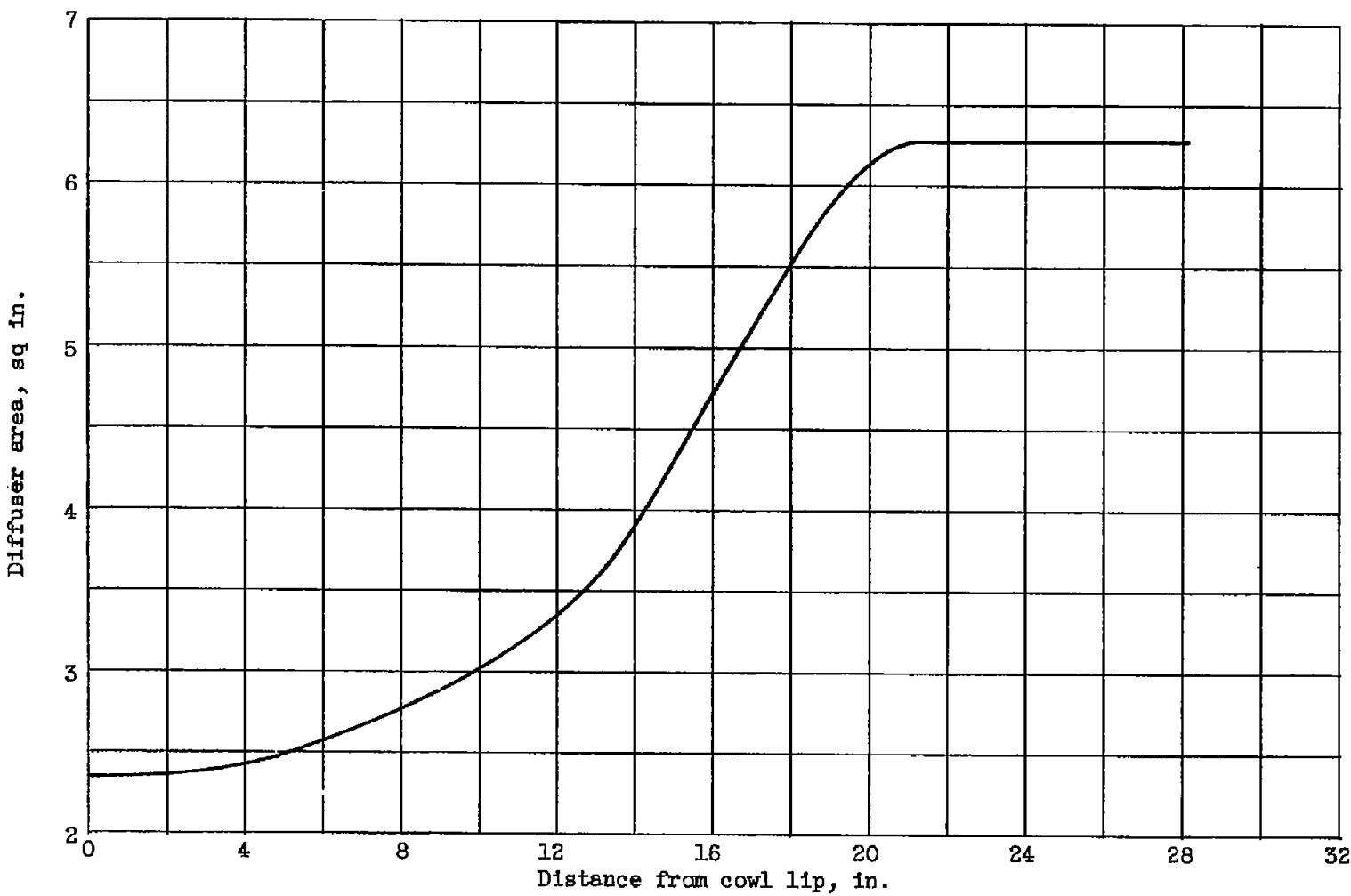
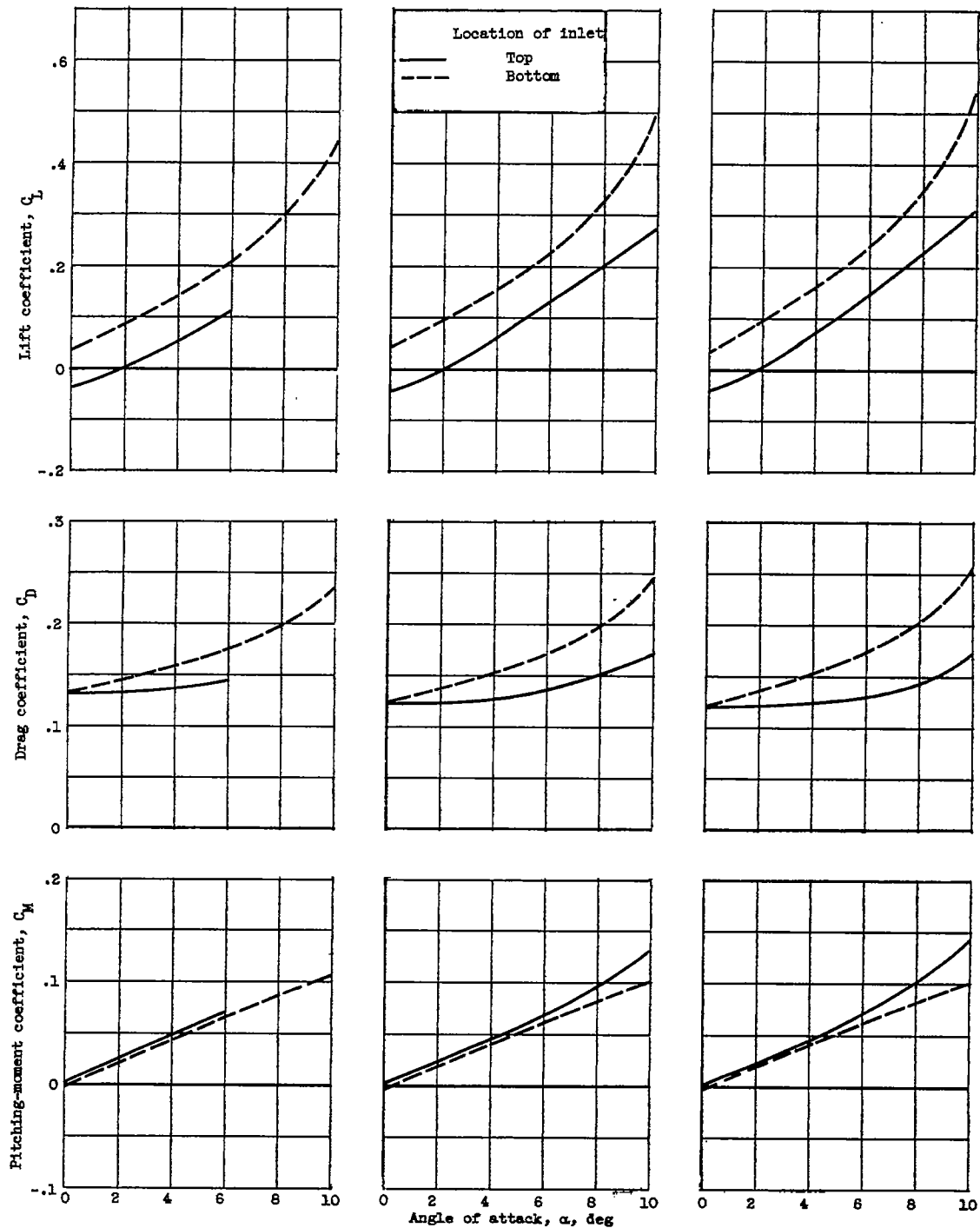


Figure 3. - Subsonic diffuser-area variation.



(a) Free-stream Mach number, 1.5. (b) Free-stream Mach number, 1.8. (c) Free-stream Mach number, 2.0.

Figure 4. - Variation of force and moment coefficients with angle of attack. (Supercritical inlet operation.)

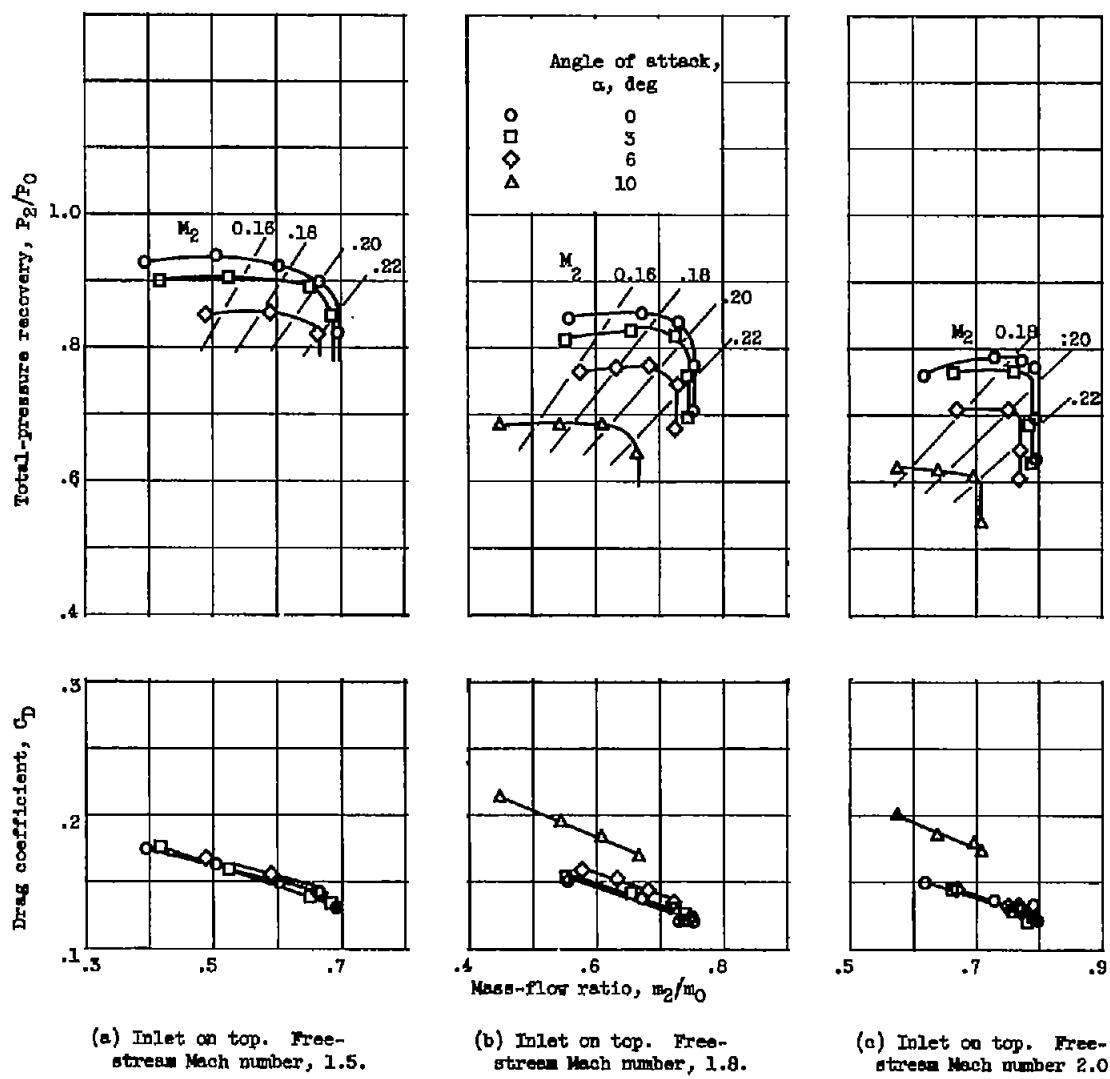
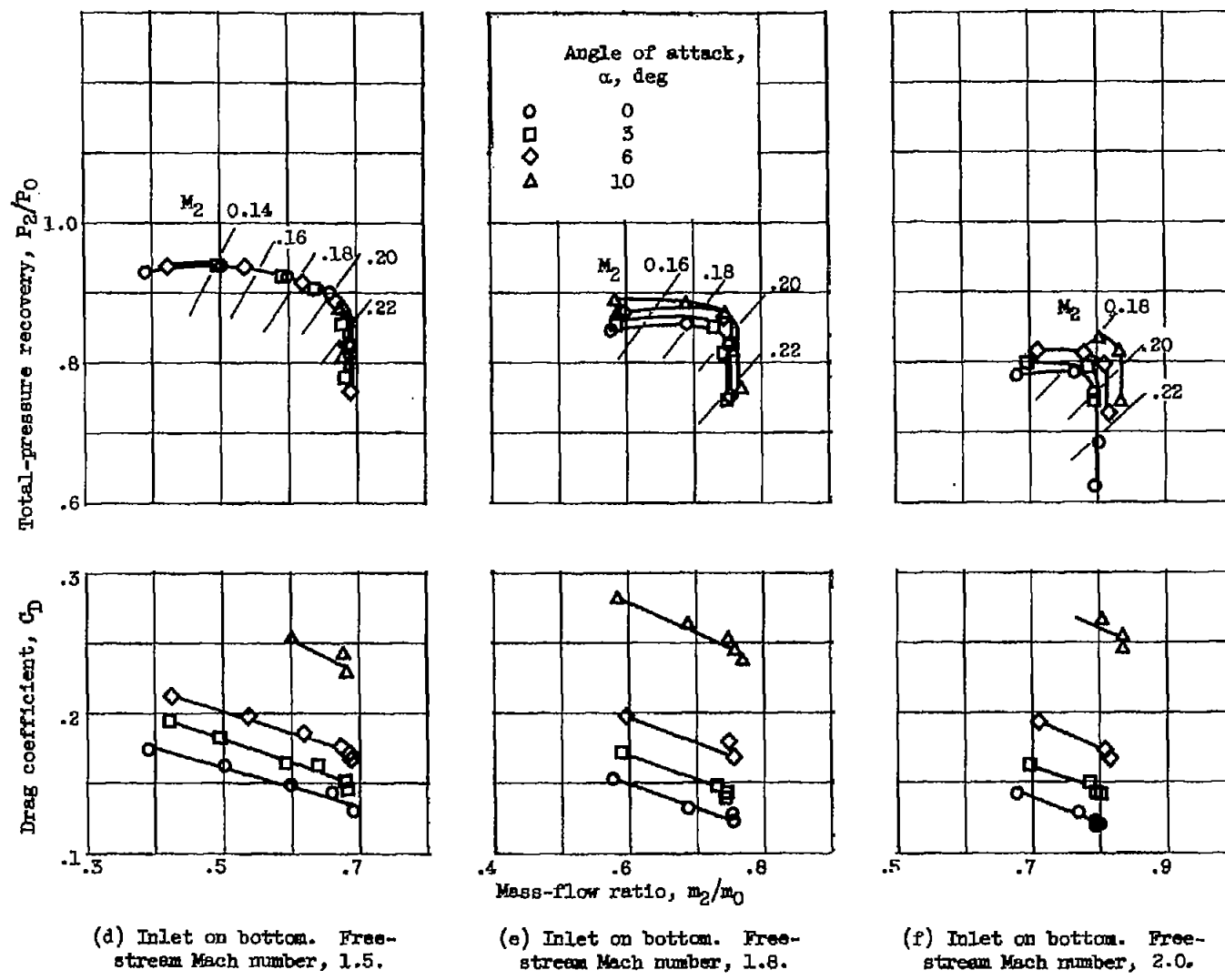


Figure 5. - Variation of pressure recovery and drag coefficient.  $M_2$ , diffuser-discharge Mach number.

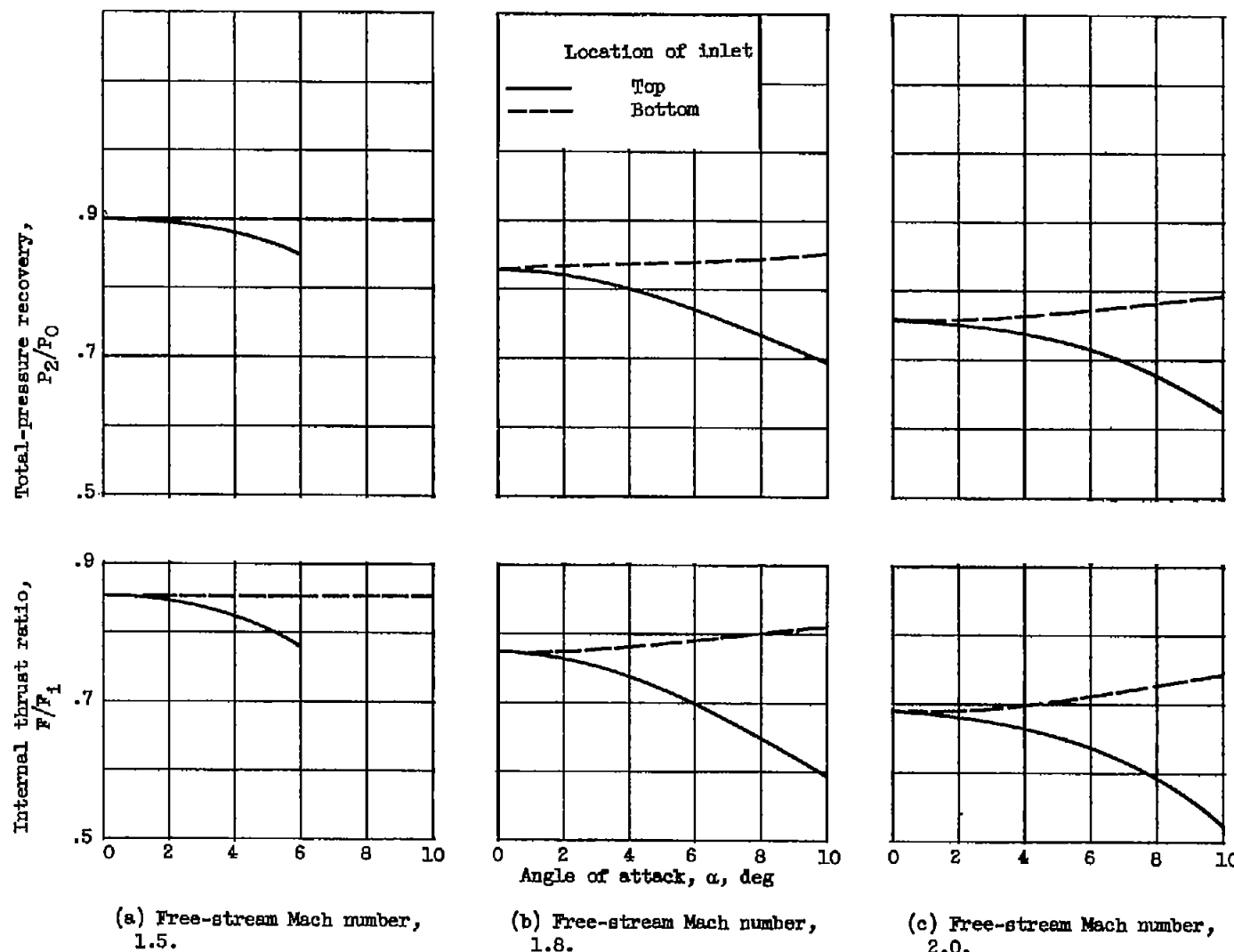


(d) Inlet on bottom. Free-stream Mach number, 1.5.

(e) Inlet on bottom. Free-stream Mach number, 1.8.

(f) Inlet on bottom. Free-stream Mach number, 2.0.

Figure 5. - Concluded. Variation of pressure recovery and drag coefficient.  $M_2$ , diffuser-discharge Mach number.



(a) Free-stream Mach number, 1.5.

(b) Free-stream Mach number, 1.8.

(c) Free-stream Mach number, 2.0.

Figure 6. - Variation of pressure recovery and internal thrust ratio. Diffuser-discharge Mach number, 0.20; altitude, 35,000 feet.

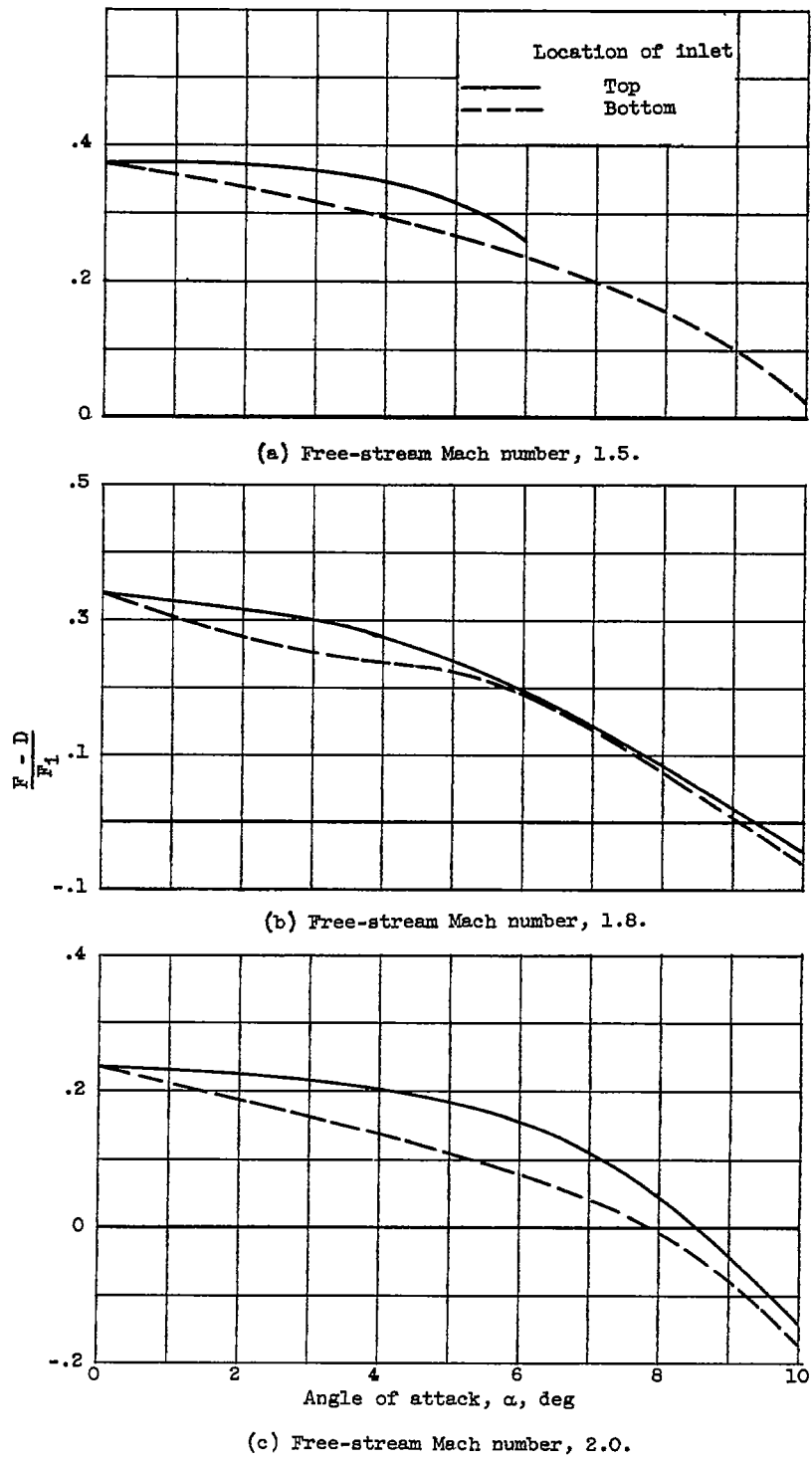


Figure 7. Ratio of thrust-minus-drag to ideal thrust.  
Diffuser-discharge Mach number, 0.20; altitude,  
35,000 feet.

3227

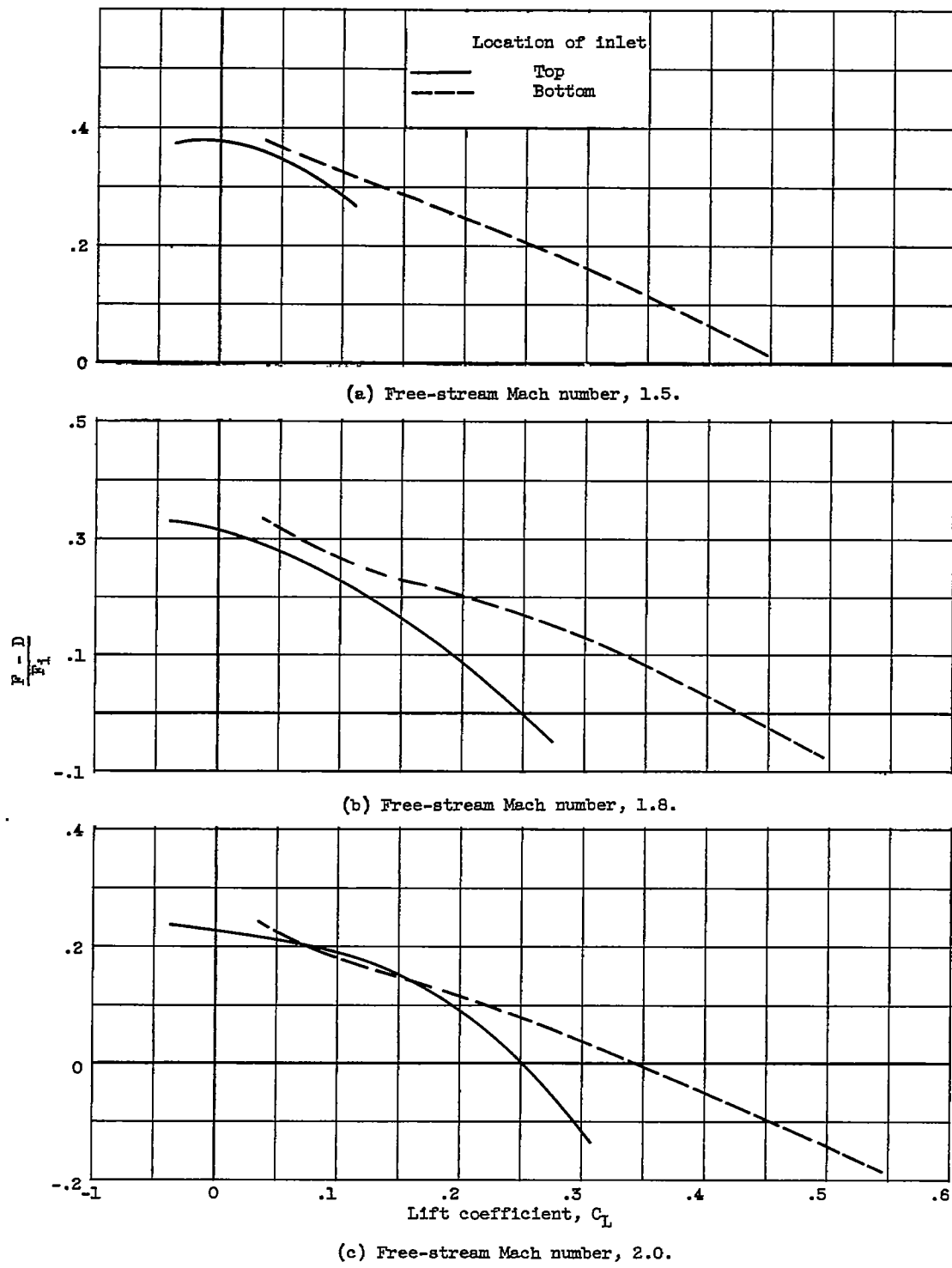


Figure 8. - Ratio of thrust-minus-drag to ideal thrust. Diffuser-discharge Mach number, 0.20; altitude, 35,000 feet.

~~CONFIDENTIAL~~

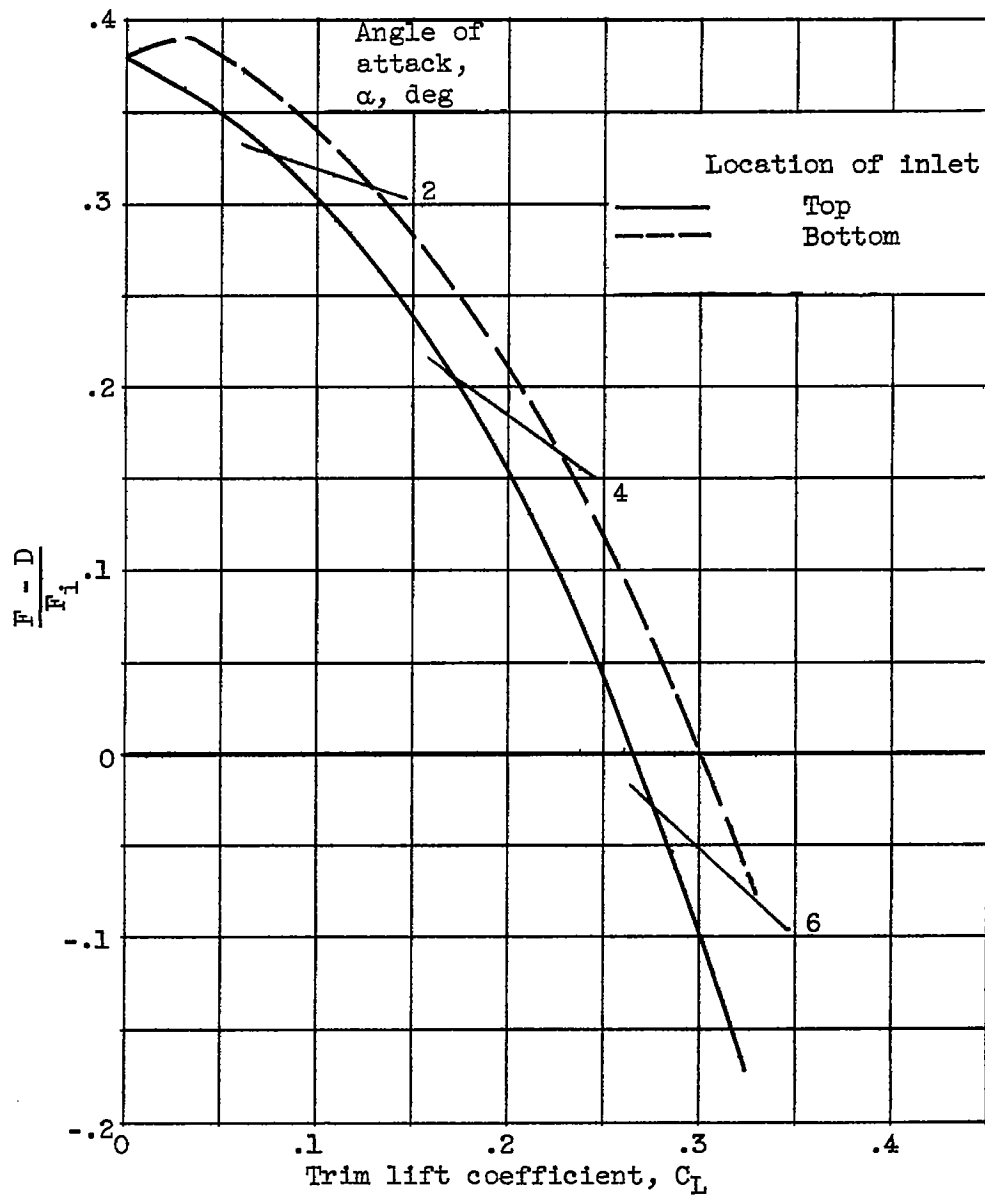


Figure 9. - Ratio of thrust-minus-drag to ideal thrust for model of reference 2.  $25^\circ$  Inlet; boundary-layer scoop-height parameter  $h/r_i$ , 0.154; free-stream Mach number, 2.0; diffuser-discharge Mach number, 0.18; altitude, 35,000 feet.